We are IntechOpen,
the world's leading publisher of
Open Access books
Built by scientists, for scientists

4,800
Open access books available

122,000
International authors and editors

135M
Downloads

Our authors are among the

154
Countries delivered to

TOP 1%
most cited scientists

12.2%
Contributors from top 500 universities

BOOK
CITATION
INDEX
CLARIVATE ANALYTICS
INDEXED

WEB OF SCIENCE™

Selection of our books indexed in the Book Citation Index
in Web of Science™ Core Collection (BKCI)

Interested in publishing with us?
Contact book.department@intechopen.com

Numbers displayed above are based on latest data collected.
For more information visit www.intechopen.com

Chapter

Rapid Evaluation of Biomass Properties Used for Energy Purposes Using Near-Infrared Spectroscopy

Jetsada Posom, Kanvisit Maraphum and Arthit Phuphaphud

Abstract

The parameters corresponding to combustion and pyrolysis such as proximate parameter (emissions), calorific value, elemental component, pyrolysis characteristics (temperature), and thermal properties are necessary to the thermal conversion process and the trading of biomass. Traditionally, these parameters of wood chips, milled wood, and biomass pellets are determined with chemicals, time-consuming, and required technical experts, such as thermogravimetry, bomb calorimetry, dry oven, muffle furnace, and so on. The near-infrared (NIR) spectroscopy is a rapid, noncontact no-chemical measurement. For NIR spectroscopy, only 2–3 seconds are used for evaluation, and it could be used for online measurement. The application of NIR spectroscopy in the estimation of the biomass characteristics of wood chips, milled wood, and biomass pellets is described in this chapter.

Keywords: biomass properties, pyrolysis characteristics, proximate analysis, calorific value, near-infrared spectroscopy

1. Introduction

Nowadays, the utilization of alternative energy is increasing because energy produced from fossil fuels increase in greenhouse gasses which lead to global warming [1, 2]. Biomass produced from fast-growing tree and waste of agricultural activity is interesting because it can be used in the future [3]. Many countries have focused on the use of biomass fuel to be the resource of future energy. Therefore, utilization with high efficiency is a key [4]. To achieve efficiency of thermal conversion process, knowledge of biomass properties used for energy purposes is important. For example, the parameters that are important for combustion are calorific value (including gross calorific (GCV) or higher heating value (HHV) and net calorific value (NCV) or lower heating value (LHV)), proximate data or emission (including moisture content (MC), volatile matter (VM), fixed carbon (FC) and ash (A)), and elemental component (carbon (C), hydrogen (H), oxygen (O), nitrogen (N), and sulfur (S)), while the important parameter for pyrolysis process is pyrolysis characteristics (temperature) (including T_{onset}, T_{sh}, T_{peak}, T_{offset}, and DTG_{peak}), kinetic parameter, proximate parameter, and elemental component. On the other hand, parameter which is essential in designing of equipment for the drying and drying

process is thermal properties (including thermal diffusivity, thermal conductivity, specific heat) [5]. These parameters are explained as follows:

1.1 Calorific value

Calorific value (CV) is the total energy released when the matter is burned. CV is divided into two types, i.e., gross calorific value (GCV) and net calorific value (NCV). CV is generally used to calculate, design, and operate thermal power plants [6]. It also can be used to interpret how biomass is used to achieve process efficiency [7, 8]. The GCV is "the amount of heat released from combustion of a certain amount of fuel and assuming its combustion product water had returned to liquid state at the end of a measurement in which it took the latent heat of vaporization of product water into account". NCV demonstrates the total of heat released under conditions where "the product water was still at vapor state and its latent heat of vaporization was not recovered" [9]. GCV is generally determined using bomb calorimetry.

Meanwhile, NCV is determined using a calculation method [10, 11] with theoretical function of the GCV by subtraction from moisture content (MC) as follows [12]:

$$NCV_{wb} = GCV_{wb} - 2.443 \times MC\% \tag{1}$$

where NCV_{wb} is the lower heating value (MJ/kg) and GCV_{wb} is the higher heating value (MJ/kg). GCV is expressed on a wet weight basis (MJ/kg). MC is percent moisture content expressed on a wet basis. Using the term NCV is better than GCV if it operates under actual operating conditions because the LHV represents a real energy content, which is defined as the efficiency of the thermal process [13].

1.2 Proximate analysis (emission)

Proximate data include four main parameters, i.e., MC, VM, FC, and Ash. MC is the amount of water in a substance which had a negative effect on the pyrolysis and combustion process, for example, a negative effect on both process and quality of bio-oil production where temperature dropped during pyrolysis and provided more water contents in bio-oil products. Measuring MC can be conducted by drying in an oven (ASTM E1756-08) [14]. VM is the vapor gas released after MC is released. Generally, VM has around 70–80% of dried biomass. VM content indicates whether the biomass was gasified easily or not and whether it was usable for boiler and gasifier design [15]. In fast pyrolysis and gasification process, VM was utilized to estimate the liquid fuel and gas fuel rate. VM was measured by muffle furnace, following the standard method of the ASTM E87282 (2006) and particular wood fuels [16]. FC is calculated by equation FC = 100-(MC% + VM% + A%) as as-received base. FC is the residue contained after MC and VM are released and mostly consists of carbon content. Ash is the solid residue after biomass volatilizes and FC is combusted [17]. High ash content leads to low HV and negative factor of storage and transportation due to no energy content. Ash content is determined using the muffle furnace method following the ASTM E1755-01 [18]. Ash content leads to trouble in waste systems due to fouling and slagging.

Normally, according to standard method, the determination of proximate analysis requires a long time which leads to cost implications [17]. Thermogravimetry (TG) can be used to determine the proximate analysis also. TG was a direct method and convenient and required small sample to be used. The direct measurement of proximate data of biomass examined by TGA is illustrated in **Figure 1**. TGA is the method utilized to study the degradation behavior in biomass burned and degraded,
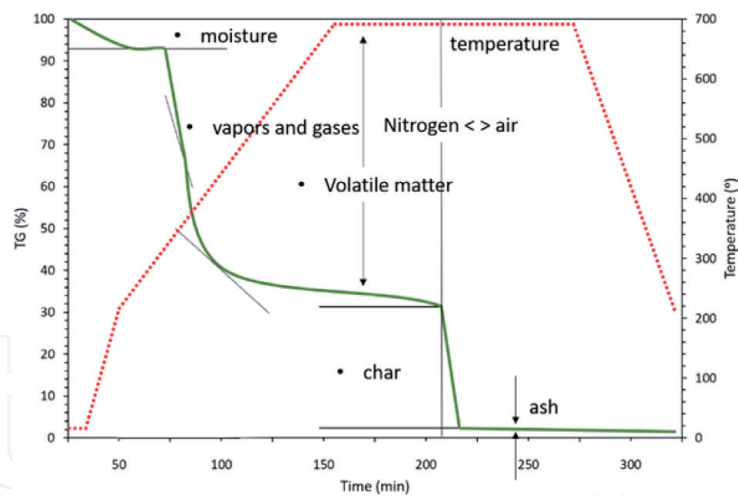
Figure 1.
Thermal behavior of biomass carried on by TGA [19].

recording weight loss as a time function versus temperature. MC, VM, FC, and A were estimated by direct measurement of weight changes from the TG chart [18].

1.3 Elemental compositions

The elemental components of biomass (i.e., C, H, N, O, and S) are defined as 100% = C + H + O + N + S + A. It is necessary in operating the overall thermal process, such as for calculation of heat content and balancing of the heat process [20]. For example, it is used to evaluate the total of flue gas (air) required to complete combustion. The burning of biomass containing more S and N leads to oxide emissions, i.e., SO_x, NO, and NO_x, released into the atmosphere, which leads to acid rain [17]. High C and H lead to increased HV, but high O content leads to decreased HV [21]. Elemental composition is determined using CHNS analyzer, which is carried on by burning a sample in a combustion chamber with pure O_2 and then measuring the gasses released (such as CO_2, N_2, SO_2, and H_2O) from combustion [20].

1.4 Pyrolysis characteristic

Pyrolysis is a thermal degradation process under the condition of absence oxygen [17], which demonstrates the behavior degradation of biomass. Pyrolysis characteristics, i.e., T_{onset}, T_{sh}, T_{peak}, T_{offset}, and DTG_{peak}, were defined as: "T_{onset} was the extrapolated onset temperature calculated from the partial peak that results from the decomposition of the hemicellulose component, T_{sh} was the temperature corresponding to the overall maximum of the hemicellulose decomposition rate, DTG_{peak} was the overall maximum of the cellulose decomposition rate (dm/dt at the highest peak, wt loss %/min), T_{peak} was the temperature corresponding to the overall maximum of the cellulose decomposition rate, and T_{offset} was the extrapolated offset temperature of the DTG_{peak} curves determined using thermogravimetric analysis (TGA)" [22]. The direct measurement of pyrolysis characteristics determined using DTG curve is shown in **Figure 2**. These parameters are applied to operate pyrolysis process [24]. T_{onset} is the start of the degradation of biomass, as it is needed to know when the biomass is degraded and to help to set the gas condensation time. T_{peak} is the maximum decomposition since the biomass that decomposed at temperature at T_{peak} can produce the highest gas production rate equaling to DTG_{peak}. The temperature of T_{offset} had no composition of biomass. If the process is heated above T_{offset}, it affects the cost of capital energy.
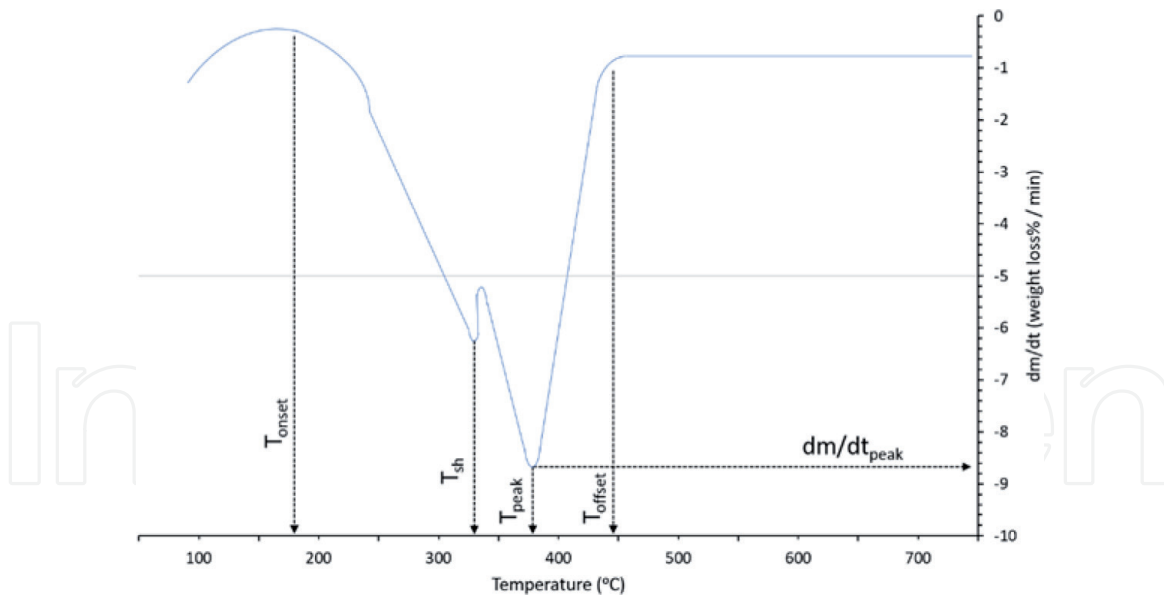
Figure 2.
DTG curve profile of milled bamboo [23].

In addition, many researchers have mentioned pyrolysis behavior as follows: Wannapeera et al. [25] and Lv et al. [26] mentioned that proportions of element compositions effect pyrolysis behavior. For example, high lignin shows slow degradation, while high hemicellulose and cellulose provide fast degradation [25, 26]. High cellulose provides high yields of bio-oil, high hemicellulose content provided high gas yields, and high lignin content provided high charcoal residue [27]. Yang et al. [28] reported that hemicellulose was degraded at 220–315°C, cellulose was decomposed at 315–400°C, and lignin was slowly degraded in a wide range between 160 and 900°C. Then, the pyrolysis behavior of biomass depends on the ratio of chemical content in biomass, such as hemicellulose, cellulose, and lignin. As such, understanding the degradation behavior is important in achieving efficiency of thermal conversion.

1.5 Kinetic parameters

Understanding of degradation behavior of biomass which explains the cracking mechanism required knowledge of kinetic behavior. Kinetic parameters, i.e., activation energy (Ea), pre-exponential factor (A), and reaction order (n) [29, 30], are employed to predict of the reaction behavior, which are usable for the optimization of the pyrolytic degradation process; they are examined using the information of biomass decomposition obtained from the thermogravimetric (TG) and derivative thermogravimetric (DTG) [29]. Kinetic parameters are utilized to design and achieve efficiency of processes [31, 32]. The minimum amount of energy needed to initiate chemical change is calculated using Ea, while the reaction rate is calculated using A and n [29].

2. Application of NIR spectroscopy on estimation of biomass properties

2.1 NIR spectroscopy for quantitative and qualitative analysis

In the 1800s, William Herschel discovered that the end of the visible band could provide heat [33]. In 1835, Ampere found that this was one of the electromagnetic

waves which have its wavelength in light. It was called infrared radiation [34]. Until in 1960, much research was reported involving IR analysis and its application. The research showed that this was a new method which could be used in evaluating water content [35]. Meanwhile, Karl H. Norris succeeded in using the spectroscopic method, for example, visible and NIR for predicting the quality of agricultural products (i.e., grains). Since 1970, many publications have reported on the application of NIR spectroscopy with food and agricultural products. This was a wide use of NIR spectroscopy. Near infrared (NIR) ranged between 700 and 2500 nm (12,500–4000 cm^{-1}) and is the technique which studies the correlation between analyte and its corresponding NIR radian [36]. NIR radian is absorbed by the chemical bonds of C–H, N–H, S–H, C=O and O–H [36]. NIR technique had many advantages, such as being rapid, nondestructive, no-chemical use, environmentally friendly, and so on.

Despite NIR having many advantages, its weakness should be not overlooked. If the concentration of analyte is lower than 0.1% of the total weight of sample, the calibration equation is acceptable [37], because the peaks of analyte are overlapped and hidden from other substances. The basic NIR spectrometer contained three parts, i.e., light source, detector, and mathematical model [36]. The assumption of NIR protocol was that if the concentration of a sample changed, the absorption of the sample may differ. Basic NIR spectroscopy creates a mathematical equation that can provide the highest performance, which is indexed by accuracy of model. The accuracy of the calibration equation is indexed by statistical terms of coefficient of determination (R^2), standard error of prediction (SEP), residue prediction deviation (RPD), and bias. The application of NIR model is indicated by R^2 and RPD. If a model provided an R^2 of between 0.50 and 0.64, it could be used toward rough screening: 0.66 and 0.81, applied for screening and approximate calibrations; 0.83 and 0.90, applied for caution with most applications; and 0.92 and 0.96, applied for most applications [38] and, for RPD, between 0.0 and 2.3, not recommended, 2.4 and 3.0 applied for very rough screening, 3.1 and 4.9 applied for screening, 5.0 and 6.4 applied for quality control, 6.5 and 8.0 applied for process control; and RPD > 8.1 applied for any application [38]. Nicolaï et al. [39] and Zornoza et al. [40] indicted that R^2 > 0.90 and RPD > 3 was an excellent prediction; 0.81 < R^2 < 0.90 and 2.5 < RPD < 3 was a good prediction, 0.66 < R^2 < 0.80 and 2.0 < RPD < 2.5 was an approximate prediction, and R^2 < 0.66 and RPD < 2 was a poor prediction. For biomass, the physical forms included ground, chipped, and pelleted. **Figure 3** shows the different physical forms of biomass used for the thermal conversion process. The NIR spectroscopy used to estimate the biomass properties coupled with various physical forms is explained in the next topic.
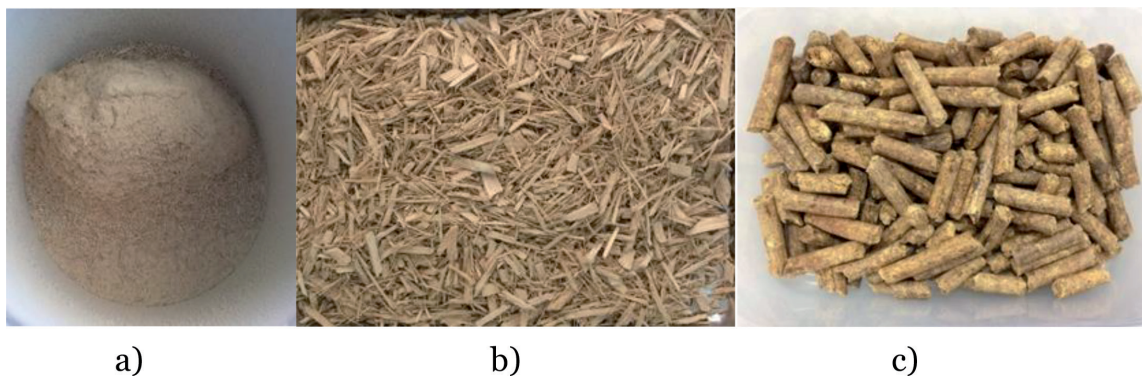

a)   b)   c)

Figure 3.
(a) Ground biomass, (b) bamboo chips format, and (c) Leucaena *pellets.*

2.2 Proximate analysis and calorific value

The prediction of biomass properties used for energy purpose using NIR spectroscopy has been utilized by many researchers, such as cassava rhizome ground (MC, HHV, and LHV) [41], maize cob (GCV) [19], and recycled sawdust (GCV and ash) [42]. The measurement of MC was conducted by Shrestha and Sirisomboon [43], predicting the MC of bamboo wood chips using two different portable spectrometers, i.e., NIR-Gun (600–1100 nm) and MicroNIR (1150–2150 nm). **Figures 4** and **5** illustrate the scanning technique of two spectrometers through diffuse reflectance mode and the particle size of bamboo wood chips, respectively. The calibration equation was developed using PLS algorithm. The statistical terms of R^2, SECV, SEP, bias, and RPD were used to examine the performance of the NIR model, providing 0.924, 2.871% wb, 2.385% wb, −0.250% wb, and 3.656 for NIR-Gun. Meanwhile, a MicroNIR spectrometer gave 0.743, 4.349% wb, 4.499% wb, 0.026% wb, and 1.972, respectively. The results indicated that the model is suitable for screening and approximating the MC in bamboo chips. This technique benefits commerce in terms of setting prices and was usable in process control using the parameter of MC such as drying process, pelletization, and combustion. Portable spectrometers are convenient to use and suitable for use on field.

Prediction of MC and HHV of pellets fuel was investigated by Posom and Sirisomboon [44], who developed the NIR model to evaluate the MC and HHV of *Leucaena* pellets using an FT near-infrared spectrometer. **Figure 6a** illustrates the scanning technique for *Leucaena* pellets (8 mm diameter). Each sample was placed
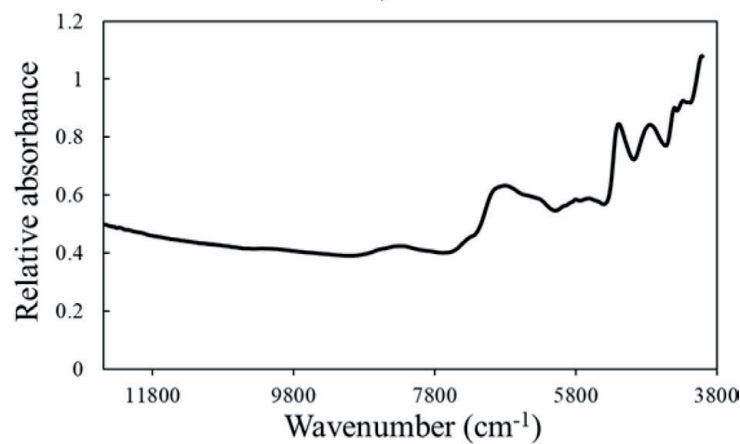

a)   b)

Figure 4.
Scanning of wood chips using portable NIR spectrometer (a) NIR-gun and (b) MicroNIR spectrometer.

Figure 5.
Particle size of bamboo wood chips.

a)

b)

Figure 6.
(a) Scanning of Leucaena *pellets in diffuse reflectance mode and (b)* Leucaena *pellets spectrum.*

in a quartz sampling cup (dimension with 87.0 mm diameter and 87.5 mm height) and scanned through the quartz window using a rotary mode. The scanning was done 64 times per sample and averaged to one spectrum. The spectrum of *Leucaena* pellets is illustrated in **Figure 6b**. In commercial setting where the MC and HHV are necessary, they are measured for quality assurance. The rapid method was used as an alternative method to the traditional MC and HHV due to complications including time, cost, and the requirement of a skilled technician. Based on quality assessment, NIR spectroscopy measured MC and HHV within 30 seconds.

For the MC model, the spectra pretreated by min-max normalization gave the affective calibration equation and wavenumber range of 7506–5446.3 and 4428–4242.9 cm^{-1}, providing the best result with a r^2 of 0.995, RMSECV of 0.187 (%wb), and RPD of 13.9. Meanwhile, the HHV model developed with the min-max normalization spectra, wavenumber range of 9403.8–7498.3, and 6102–5446.3 cm^{-1} also provided the optimal model, with r^2 of 0.964, RMSECV of 89.2 J/g, and RPD of 4.71. The MC and HHV models were excellent for any application.

Posom and Sirisomboon [45] developed the mathematical equation for the prediction of HHV, VM, FC, and ash of ground bamboo. Milled bamboo (particle size ≤3 mm (see **Figure 4a**)) was scanned using FT-NIR spectroscopy with diffuse reflectance mode. The absorbance was recorded by log 1/R unit, where R is the reflectance of milled sample. The purpose was to apply the NIR technique instead of bomb calorimetry and thermogravimetry (TG). The model was optimized using PLS regression. The result of HHV, VM, FC, and ash model provided r^2 of 0.92, 0.82, 0.85, and 0.51; RMSEP of 122 J g^{-1}, 1.15, 1.00, and 0.77%; and RPD of 3.66, 2.55, 2.62, and 1.44, respectively. The summary was that NIR spectroscopy was successful in estimating the HHV, VM, and FC; meanwhile the ash model was not recommended because of low RPD. It was recommended that the range of reference value should be as wide as possible. The spectra of the ground sample can give a high precision because of homogeneous sample. However, the use of ground sample was complicated in terms of sample preparation, which led to higher time and cost. Posom and Sirisomboon [46] updated the NIR model in prediction of HHV, LHV, MC, VM, FC, and ash of bamboo wood chips (see **Figure 4b**). This model replaced the previous model (ground bamboo model). The samples were collected for two seasons in 2017 and 2018. In real situations, wood chip preparation is easier than ground sample. In addition, even though the previous study on ground bamboo reported a good performance, in the prediction of ground sample, it was found to be inconvenient because of complicated sample preparation. NIR model were developed by directly scanning bamboo chips and created based on PLS regression. A big particle size led to lower spectrum repeatability, but this problem was solved using spectral preprocessing. The improvement of MC, ash, VM, and FC models (bamboo chips) could be applied for quality assurance. The HHV and LHV models can be utilized in most applications. A big particle size of wood chips can affect negatively in the calibration equation because the sample was inhomogeneous; however, this problem can be solved by spectral pretreatment technique. Therefore, the direct scanning in wood chips can eliminate the need process for grinding wood samples [46]. Moreover, a calibration equation can predict ash content in bamboo wood chips successfully. The reason why NIR spectroscopy can predict ash content is because: "the infrared bands for inorganic materials are broader, fewer in number and appear at lower wavenumbers than those observed in organic materials, and if an inorganic compound forms covalent bonds within an ion, it can produce a characteristic infrared spectrum" [47].

The heating value and proximate analysis (MC, VM, FC, and A model) model of biomass pellets was studied by Feng et al. [24], who constructed a 2D NIR hyperspectral image in the prediction of proximate analysis and illustrated a quality distribution map. The rapid measurements for properties of biomass pellets helped to monitor the feedstock pellet production. The models were constructed using an algorithm of PLSR and least-squares support-vector machine (LSSVM). The optimized calibration models constructed by successive projections algorithm (SPA)-LSSVM gave excellent efficiency in the prediction of MC, A, VM, and HV, with the R^2 of 0.94, 0.92, 0.94, and 0.90, respectively. The quality indexes of pellets can be visualized on predicting component maps by calculating prediction value to each pixel into the 2D hyperspectral images.

Nakawajana et al. [11] predicted the HHV, LHV, and ash of milled rice husk using FT-NIR spectroscopy. Illustrations of pure cellulose, lignin, and sample spectrum are displayed in **Figure 7**. Vibration band of cellulose (range 1) and lignin (range 2) was quite different, and some wavelengths of risk husk were quite similar to cellulose and lignin. The fact was that the rice husk contains lignocellulose. Range 1 was the vibration band of cellulose, and range 2 was the vibration band of lignin. Therefore, if we want to know which wavelength is the vibration band of analyte,
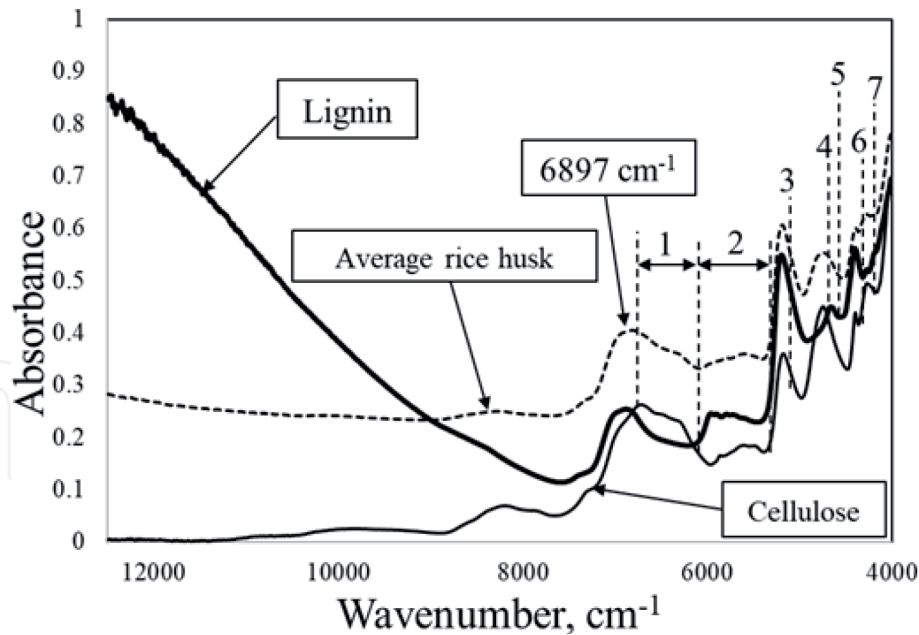
Figure 7.
Average rice husk, hemicellulose, cellulose, and lignin spectrum [11].

scanning of pure analyte with NIR radian should be taken to find obvious peaks in the absorption spectrum. We can assume that an obvious peak is the vibration band of analyte, which is suitable for model development. The calibration equation was validated by an unknown sample, which was obtained from another mill rice plant. The unknown sample was collected from different resources to set calibration. It ensured that the developed model could be used for future samples. HHV (J/g) was determined using bomb calorimeter, and LHV can be calculated using the knowledge of HHV and MC (%wet basis). LHV_{wb} was then determined as follows [7]:

$$LHV = HHV - 2433 \times MC \qquad (2)$$

2443 is the latent heat of the vaporization of water at 25°C (J/g), and MC was the unit on a %wb determined from the air dry oven.

Ash content was determined using bomb calorimeter. It was the solid residue after the sample burned and was calculated as follows:

$$A (\%wt) = W_a/W_s \times 100 \qquad (3)$$

W_a is the weight of the sample after burned, and W_s is the initial weight. The outliers were checked and removed using equation $\frac{(X_i - \overline{X})}{SD} \geq \pm 3$, where X_i is the reference value of sample i. X and SD are the mean and standard deviation of reference value, respectively. If any samples satisfied the criteria, they were cut from the data set. The result provides the relative standard error of prediction (RSEP) of 1.104, 1.159, and 5.975% for HHV, LHV, and A models. The results were recommended for screening as a quality assurance. The RSEP was the relative ratio between the absolute error of prediction and measured value; an RSEP of around 5% meant that every predictive value could provide the error of approximately 5% of reference value [48].

2.3 Elemental components

Posom and Sirisomboon [10] developed the NIR model to predict C, H, N, O, and S across FT-NIR spectroscopy. The scanning of samples was conducted with
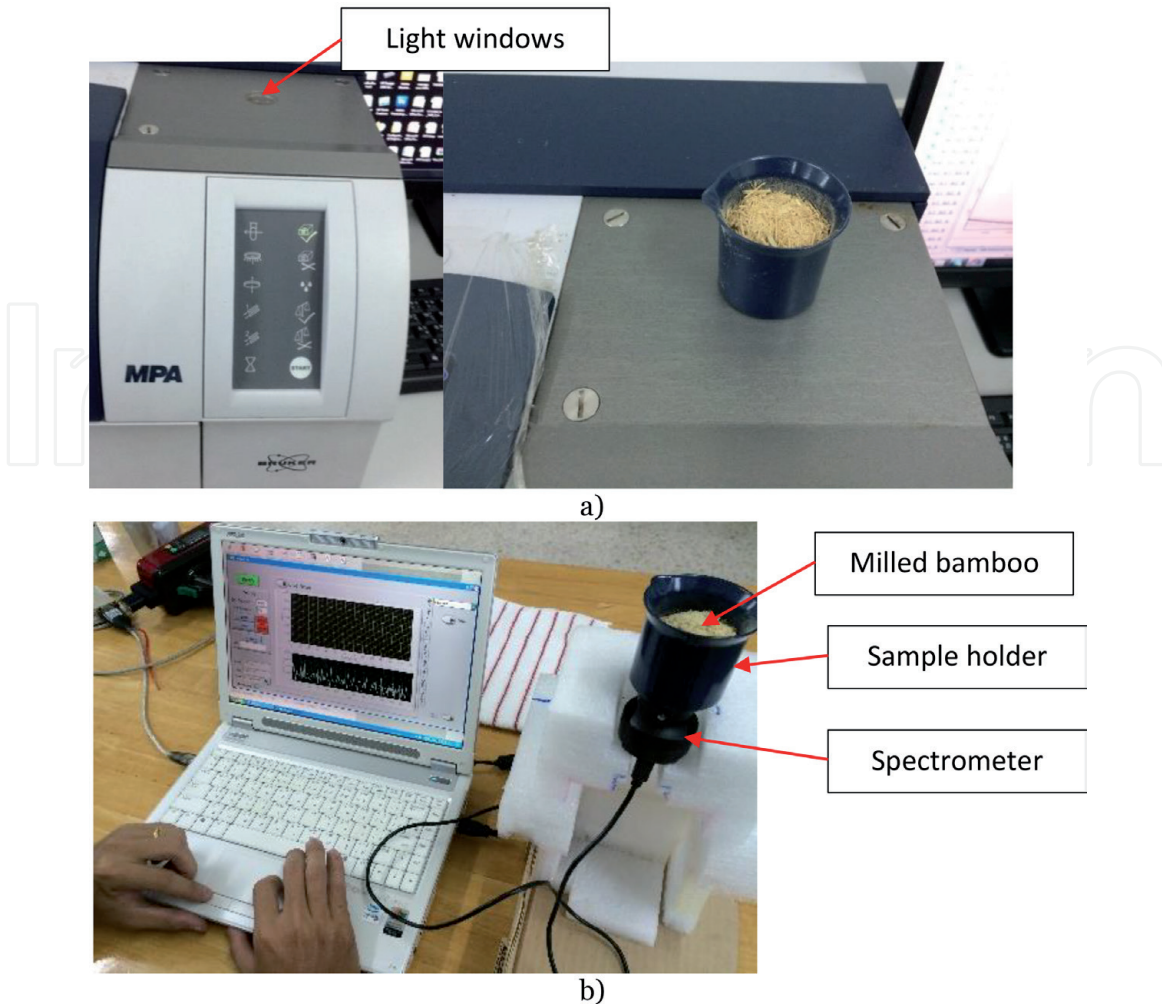
Figure 8.
Scanning of milled bamboo using (a) FT-NIR and (b) MicroNIR spectrometer.

diffuse reflectance mode, shown in **Figure 8a**. The ground sample was placed in a sample cup (43 mm diameter and 50 mm height). The bottom of the sample cup was made from quartz. The sample was scanned in diffuse reflectance mode 64 times and averaged to one spectrum. The sample at the bottom of the sample cup was obtained to be analyzed by traditional method. The model was established using PLS regression. The NIR models of C, H, N, S, and O provided r^2 and RPD of 0.803 and 2.31, 0.856 and 2.65, 0.973 and 6.6, 0.785 and 2.19, and 0.522 and 1.46, respectively. N and H model could be utilized for most applications. C and S models were fair. The O model was poor because the reference method was not precise. The reference method for O was calculated as O% = 100-C%-H%-N%-S%-Ash%, meaning that the predicted O included total error from another parameter. This result could be used to guide operation control into the thermal conversion process to predict flow rate of flue gas and air requirement in combustion and to predict flue gas component in combustion and pyrolysis. Posom and Saechua [49] predicted the elemental components (C, H, N, O, and S) of ground bamboo using low-cost spectrometer (MicroNIR spectrometer), which was a handheld spectrometer. **Figure 8b** displays the scanning method using a portable NIR spectrometer. It shows that only C (carbon) model was recommend for screening because the spectrum collected from the low-cost spectrometer was scanned once, while FT-NIR spectrometer scanned each sample for 64 times which was averaged.

2.4 Kinetic parameters

The activation energy (Ea) of ground bamboo was studied using online NIR spectroscopic method [48]. The online systems are shown in **Figure 9**, including NIR spectrometer (MicroNIR), computer, and conveyer belt. The main work was to evaluate the Ea of ground bamboo through real-time monitoring. The Ea value was determined using the Coats-Redfern method. The online prediction of Ea of the reaction order (n) at n = 1 and n ≠ 1 was investigated. The model of online measurement was created using PLS algorithm. The model of Ea at n = 1 and Ea at n ≠ 1 had r^2 of 0.781 and 0.714, respectively, and SEP of 5.249 and 6.858 kJ/mol, respectively. Both models were fair and could be applied to screening and monitoring. The vibration bands of lignocellulosic such as CH_2, hemicellulose, cellulose, and lignin influence prediction.

2.5 Pyrolysis characteristics

The identification of the pyrolysis characteristics of milled bamboo using NIR spectroscopy was conducted [23] using a FT-NIR spectroscopy, including T_{onset}, T_{sh}, T_{peak}, T_{offset}, and DTG_{peak}. The scanning method was performed using diffuse reflectance mode, which is shown in **Figure 8a**. "T_{onset} is the extrapolated onset temperature that is calculated from the partial peak resulting from the decomposition of the hemicellulose component; T_{sh} is the temperature corresponding to the overall maximum of the hemicellulose decomposition rate; DTG_{peak} is the overall maximum of the cellulose decomposition rate; T_{peak} is the temperature corresponding to the overall maximum of the cellulose decomposition rate; T_{offset} is the extrapolated offset temperature of the DTG_{peak} curves determined using thermogravimetric analysis (TGA)." The aim is to be used as an alternative for thermogravimetry method. The calibration equations were created by PLSR and validated using test set method. The results found that the models of T_{onset}, T_{sh}, T_{peak}, T_{offset}, and DTG_{peak} showed R^2 of 0.566, 0.845, 0.917, 0.973, and 0.671; RMSEP of 9.7 C, 4.36 C, 3.77 C, 2.66 C, and 0.428 wt loss %/min; and RPD of 1.52, 2.58, 3.48, 3.55, and 1.75, respectively. The vibration bands of water and hydrocarbon (CH_3, O-H stretch, Ar-OH, CH_2 and HC=CH, O-H and C-H, CH_2) influence the prediction.

2.6 Prediction of thermal properties

The use of NIR spectroscopy in the prediction of the thermal properties (thermal diffusivity, thermal conductivity, specific heat) of *Jatropha* kernels was studied by
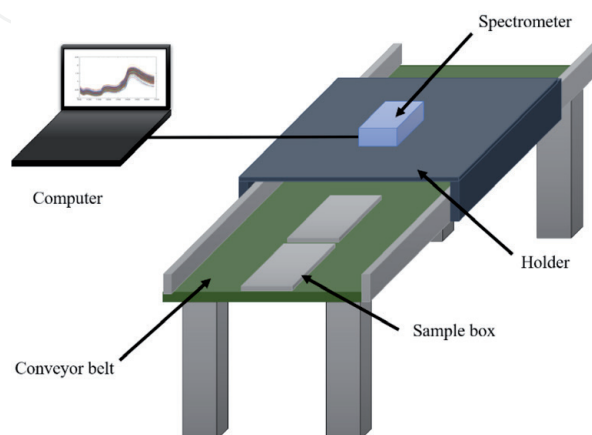

Figure 9.
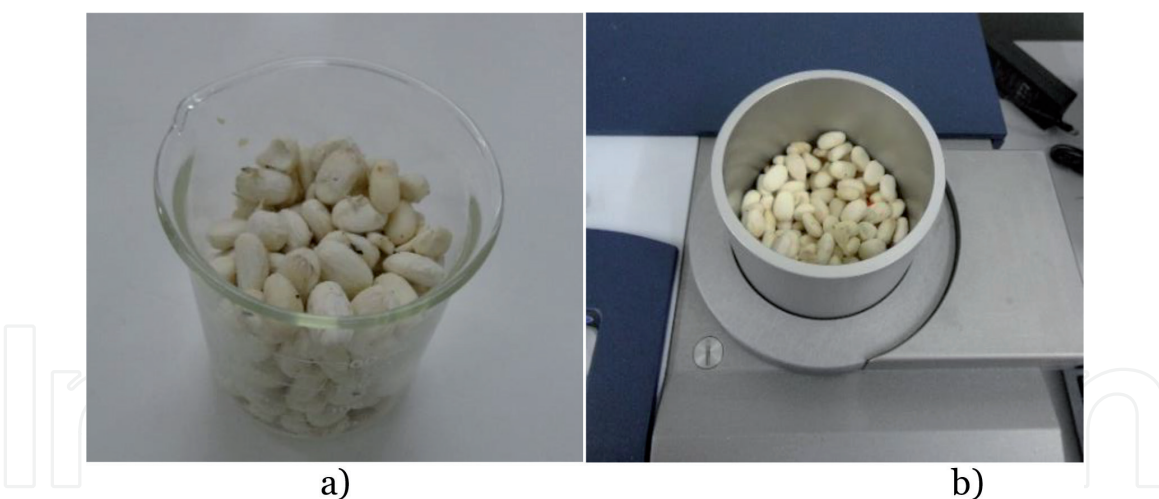*Schematic diagram of the experimental design [48].*

Figure 10.
(a) Jatropha *kernels, (b) rotational diffuse reflectance scanning.*

Posom and Sirisomboon [50]. The samples were scanned using FT-NIR spectrometry across a wavenumber of 12,500–4000 cm^{-1}, with diffuse reflectance model. For the diffuse reflectance method, the scanning could confirm that there was not light transmitted through the sample. The thickness of the sample path should be enough. The calibration equations were created by PLS regression. **Figure 10a** and **b** shows *Jatropha* kernels and scanning of technique, respectively. The results of thermal diffusivity, thermal conductivity, and specific heat at 40 and 100°C had the R^2 of 0.5968, 0.7592, 0.7509, 0.4211, and 0.6396%, respectively; the RMSEP of 1.1 × 10^{-6} m^2 s^{-1}, 0.0169 W m^{-1}°C^{-1}, 0.0685 W m^{-1}°C^{-1}, 5.88 kJ kg^{-1}°C^{-1}, and 15.8 kJ kg^{-1}°C^{-1}; the biases of −2.52 × 10^{-7} m^2 s^{-1}, 2.85 × 10^{-3} W m^{-1}°C^{-1}, 2.52 × 10^{-2} W m^{-1}°C^{-1}, 1.83 kJ kg^{-1}°C^{-1}, and 4.69 kJ kg^{-1}°C^{-1}; and RPD of 1.57, 2.04, 1.98, 1.28, and 1.64, respectively. NIR spectroscopy could be applied in the estimation of the thermal properties of *Jatropha* kernels, due to reduced times and costs. The use of NIR spectroscopy required only 2–3 minutes for measuring and can be applied for drying process control.

3. Caution in model development and application

Even through the NIR spectroscopy is rapid, environmental friendly, and low cost in long-term analysis, the application of NIR spectroscopy should be careful as follows: if the concentration of analyte has lower than 0.1% of the total concentration of the sample, the calibration equation was not acceptable [37] because the absorption peak of the analyte is overlapped by other peaks; the model could be updated monthly to reduce the impact of season; dark and white reference collection of NIR instrument should be done often during operation.

For model development, the caution is before model development, the repeatability and reproducibility of reference method could be firstly examined until the result is satisfied; the maximum R$^2_{max}$ could be calculated before modeling; the calibration equation could be validated again using unknown sample in which that sample must be obtained from different areas and different seasons unless there are three seasons.

4. Conclusion

From previous study, many research demonstrated that this technology is suitable in predicting biomass quality; it is usable in commercial and process control.

NIR spectroscopy is rapid which has the ability in the evaluation of the proximate data. A good prediction was found in predicting HHV ($r^2 > 0.9$), MC ($r^2 > 0.9$), VM ($r^2 > 0.8$), and FC ($r^2 > 0.8$), which is suitable toward for any application [38]. The performance of the model will be good when the range of analyte developed is wide.

For evaluation of elemental component, a good performance was found in the prediction of C ($r^2 > 0.8$), H ($r^2 > 0.8$), and N ($r^2 > 0.8$), which could be utilized for most application [38]. A poor prediction is found in the prediction of O and S, which is not recommended. The O model is low performance due to its reference method which is not precise (calculation method), while the S model is low performance because its range is not narrow which seems that the S content in biomass is not different.

The pyrolysis characteristic model was a good accuracy for the prediction of T_{sh} ($r^2 = 0.845$), T_{peak} ($r^2 = 0.917$), and T_{offset} ($r^2 = 0.973$). This method is rapid (2–3 seconds per sample), which is usable in the process control of pyrolysis.

For the measurement of Ea with online NIR spectroscopic method [48], it could be used as an alternative technique to TGA and Coats-Redfern method. The model is fair and could be applied for screening, which is usable to process control. The vibration bands of CH_2, hemicellulose, cellulose, and lignin impact in prediction.

Conflict of interest

The authors declare no conflict of interest.

Author details

Jetsada Posom[1,2,3*], Kanvisit Maraphum[1,2,3] and Arthit Phuphaphud[1,2,3]

1 Department of Agricultural Engineering, Khon Kaen University, Khon Kaen, Thailand

2 Applied Engineering for Important Crops of the North East Research Group, Khon Kaen University, Khon Kaen, Thailand

3 Bio-Sensing and Field Robotic Laboratory, Khon Kaen University, Khon Kaen, Thailand

*Address all correspondence to: jetspo@kku.ac.th

IntechOpen

References

[1] Taner T. Economic analysis of a wind power plant: A case study for the Cappadocia region. Journal of Mechanical Science and Technology. 2018;**32**(3):1379-1389

[2] Taner T, Naqvi SAH, Ozkaymak M. Techno-economic analysis of a more efficient hydrogen generation system prototype: A case study of PEM electrolyzer with Cr-C coated SS304 bipolar plates. Fuel Cells. 2019;**19**(1):19-26

[3] Taner T. A flow channel with nafion membrane material design of PEM fuel cell. Journal of Thermal Engineering. 2019;**5**(5):456-468

[4] Taner T, Demirci OK. Energy and economic analysis of the wind turbine Plant's draft for the Aksaray City. Applied Ecology and Environmental Sciences. 2014;**2**(3):82-85

[5] Sirisomboon P, Posom J. Thermal properties of *Jatropha curcas* L. kernels. Biosystems Engineering. 2012;**113**:402-409

[6] Nhuchhen DR. Prediction of carbon, hydrogen, and oxygen compositions of raw and torrefied biomass using proximate analysis. Fuel. 2016;**180**:348-356

[7] Werther J, Saenger M, Hartge EU, Ogada T, Siagi Z. Combustion of agricultural residues. Progress in Energy and Combustion Science. 2000;**26**:1-27

[8] Sheng C, Azevedo JLT. Estimating the higher heating value of biomass fuels from basic analysis data. Biomass and Bioenergy. 2005;**28**:499-507

[9] Shi H, Mahinpey N, Aqsha A, Silbermann R.Characterization, thermochemical conversion studies, and heating value modeling of municipal solid waste. Waste Management. 2016;**48**:34-47

[10] Posom J, Sirisomboon P. Evaluation of lower heating value and elemental composition of bamboo using near infrared spectroscopy. Energy. 2017;**121**:147-158

[11] Nakawajana N, Posom J, Paeoui J. Prediction of higher heating value, lower heating value and ash content of rice husk using FT-NIR spectroscopy. Engineering Journal. 2018;**22**(5):45-56

[12] Komilis D, Kissas K, Symeonidis A. Effect of organic matter and moisture on the calorific value of solid wastes: An update of the Tanner diagram. Waste Management. 2014;**34**:249-255

[13] Cooper CD, Kim B, MacDonald J. Estimating the lower heating values of hazardous and solid wastes. Journal of the Air and Waste Management Association. 1999;**49**

[14] ASTM E1756-08 Standard Test Method for Determination of Total Solids in Biomass. USA: ASTM International; 2008

[15] Jameel H, Keshwani DR, Carter SF, Treasure TH. Thermochemical conversion of biomass to power and fuel. In: Cheng J, editor. Biomass to Renewable Energy Process. USA: CRC Press; 2010

[16] ASTM E872-82. Standard Test Method for Volatile Matter in the Analysis of Particulate Wood Fuels. USA: ASTM International; 2006

[17] Basu P. Biomass gasification and pyrolysis: Practical design and theory. In: Biomass Characteristics. USA: Academic Press is an Imprint of Elsevier; 2010

[18] ASTM E1755-1. Test Method for Ash in Biomass. USA: ASTM International; 2007

[19] Posom J, phuphanutada J, Lapcharoensuk R. Gross calorific and ash content assessment of recycled sawdust from mushroom cultivation using near infrared spectroscopy. MATEC Web of Conferences. 2018;**192**:03021

[20] Zhang K, Zhou L, Brady M, Xu F, Yu J, Wang D. Fast analysis of high heating value and elemental compositions of sorghum biomass using near-infrared spectroscopy. Energy. 2017;**118**:1353-1360

[21] Runge TM, Zhang C, Mueller J, Wipperfurth P. Economic and environmental impact of biomass types for bioenergy power plants. In: Environmental and Economic Research and Development Program. 2013. Available from: https://www.focusonenergy.com/sites/default/files/research/1010RungeFinalReportx.pdf

[22] El-Sayed SA, Mostafa ME. Pyrolysis characteristic and kinetic parameters determination of biomass fuel powders by differential thermal gravimetric analysis (TGA/DTG). Energy Conversion and Management. 2014;**85**:165-172

[23] Posom J, Saechua W, Sirisomboon P. Evaluation of pyrolysis characteristics of milled bamboo using near-infrared spectroscopy. Renewable Energy. 2017;**103**:653-665

[24] Feng X, Yu C, Shu Z, Liu X, Yan W, Zheng O, et al. Rapid and non-destructive measurement of biofuel pellet quality indices based on two-dimensional near infrared spectroscopic imaging. Fuel. 2018;**228**:197-205

[25] Wannapeera J, Worasuwannarak N, Pipatmanomai S. Product yields and characteristics of rice husk, rice straw and corncob during fast pyrolysis in a drop-tube/fixed-bed reactor. Songklanakarin Journal of Science and Technology. 2008;**30**(3):393-404

[26] Lv D, Xu M, Liu X, Zhan Z, Li Z, Yao H. Effect of cellulose, lignin, alkali and alkaline earth metallic species on biomass pyrolysis and gasification. Fuel Processing Technology. 2010;**91**:903-909

[27] Stefanidis SD, Kalogiannis KG, Iliopoulou EF, Michailof CM, Pilavachi PA, Lappas AA. A study of lignocellulosic biomass pyrolysis via the pyrolysis of cellulose, hemicellulose and lignin. Journal of Analytical and Applied Pyrolysis. 2014;**105**:143-150

[28] Yang H, Yan R, Chen H, Lee DH, Zheng C. Characteristics of hemicellulose, cellulose and lignin pyrolysis. Fuel. 2007;**86**:1781-1788

[29] Parthasarathy P, Narayanan KS, Arockiam L. Study on kinetic parameters of different biomass samples using thermo-gravimetric analysis. Biomass and Bioenergy. 2013;**58**:58-66

[30] Syed S, Qudaih R, Talab I, Janajreh I. Kinetics of pyrolysis and combustion of oil shale sample from thermogravimetric data. In: The 7th Jordanian International Engineering Conference JIMEC'7; 27-29 September 2010; Amman-Jordan; 2010

[31] Ceylan S, Topçu Y. Pyrolysis kinetics of hazelnut husk using thermogravimetric analysis. Bioresource Technology. 2014;**156**:182-188

[32] Lopez-Velazquez MA, Santes V, Balmaseda J, Torres-Garcia E. Pyrolysis of orange waste: A thermo-kinetic study. Journal of Analytical and Applied Pyrolysis. 2013;**99**:170-177

[33] Næs T, Isaksson T, Fearn T, Davies T. Multivariate Calibration and

Classification. Chichester: NIR Publication; 2004. 323 p

[34] Davies AMC. An Introduction to Near Infrared (NIR) Spectroscopy. 2017. Available from: https://www.impublications.com/content/introduction-near-infrared-NIR-spectroscopy

[35] Osborne BG, Fearn T. Near Infrared Spectroscopy in Food Analysis. Theory of Near Infrared Spectroscopy. New York, USA: Longman Scientific & Technical; 1986. pp. 36-40

[36] Osborne BG, Fearn T. Near Infrared Spectroscopy in Food Analysis. Theory of Near Infrared Spectroscopy, USA, 133. New York: Longman Scientific & Technical; 1986. pp. 36-40

[37] Burns DA, Ciurczak EW, editors. Handbook of Near-Infrared Analysis. New York, NY: Marcel Dekker Inc; 1992. p. 13

[38] Williams P. Near-Infrared Technology-Getting the Best Out of Light. Nanaimo, British Columbia, and Winnipeg, Manitoba, Canada: PDK Grain; 2007

[39] Nicolaï BM, Beullens K, Bobelyn E, Peirs A, Saeys W, Theron KI, et al. Nondestructive measurement of fruit and vegetable quality by means of NIR spectroscopy: A review. Postharvest Biology and Technology. 2007;**46**:99-118

[40] Zornoza R, Guerrero C, Mataix-Solera J, Scow KM, Arcenegui V, Mataix-Beneyto J. Near infrared spectroscopy for determination of various physical, chemical and biochemical properties in Mediterranean soils. Soil Biology and Biochemistry. 2008;**40**(7):1923-1930

[41] Nakawajana N, Posom J. Comparison of analytical ability of PLS and SVM algorithm in estimation of moisture content, higher heating value, and lower heating value of cassava rhizome ground using FTNIR spectroscopy. IOP Conference Series: Earth and Environmental Science. 2019;**301**:012032

[42] Posom J, Nakawajana N. Gross calorific value estimation for milled maize cob biomass using near infrared spectroscopy. MATEC Web of Conferences. 2018;**192**:03022

[43] Shrestha A, Panmanas Sirisomboon P. Rapid evaluation of moisture content in bamboo chips using diode array near infrared spectroscopy. MATEC Web of Conferences. 2018;**192**:03020

[44] Posom J, Shrestha A, Saechua W, Sirisomboon P. Rapid non-destructive evaluation of moisture content and higher heating value of *Leucaena leucocephala* pellets using near infrared spectroscopy. Energy. 2016;**107**:464-472

[45] Posom J, Sirisomboon P. Evaluation of the higher heating value, volatile matter, fixed carbon and ash content of ground bamboo using near infrared spectroscopy. Journal of Near Infrared Spectroscopy. 2017;**25**(5):301-310

[46] Sirisomboon P, Funke A, Posom J. Improvement of proximate data and calorific value assessment of bamboo through near infrared wood chips acquisition. Renewable Energy. 2020;**147**:1921-1931

[47] Stuart B, Molecules I. Infrared Spectroscopy: Fundamentals and Applications. The Atrium, Southern Gate, Chichester, West Sussex, England: John Wiley & Sons, Ltd; 2004

[48] Sirisomboon P, Posom J. On-line measurement of activation energy of ground bamboo using near infrared spectroscopy. Renewable Energy. 2019;**133**:480-488

[49] Posom J, Saechua W. Prediction of elemental components of ground

bamboo using micro-NIR spectrometer.
In: Proceedings of the IOP Conference on
Earth and Environmental Science. 2019

[50] Posom J, Sirisomboon P. Evaluation
of the thermal properties of *Jatropha
curcas* L. kernels using near-infrared
spectroscopy. Biosystems Engineering.
2014;**125**:45-53